SAN098-1105C
SAND--98-1105C

CHARACTERIZATION OF LOW-MELTING ELECTROLYTES FOR POTENTIAL GEOTHERMAL BOREHOLE POWER SUPPLIES: THE LiBr-KBr-LiF EUTECTIC

CONF-980504--

Ronald A. Guidotti and Frederick W. Reinhardt
Sandia National Laboratories
P.O. Box 5800,
Albuquerque, NM 87185-0614

RECEIVED
JUN 02 1998
OSTI

ABSTRACT

The suitability of modified thermal-battery technology for use as a potential power source for geothermal borehole applications is under investigation. As a first step, the discharge processes that take place in LiSi/LiBr-KBr-LiF/FeS_2 thermal cells were studied at temperatures of 350°C and 400°C using pelletized cells with immobilized electrolyte. Incorporation of a reference electrode allowed the relative contribution of each electrode to the overall cell polarization to be determined. The results of single-cell tests are presented, along with preliminary data for cells based on a lower-melting CsBr-LiBr-KBr eutectic salt.

INTRODUCTION

Currently, modified Li/$SOCl_2$ cells are used for powering instrumentation used in deep geothermal boreholes. These cells are rated for operation up to 180°C, but due to temperature limitations, they must be insulated from the immediate thermal environment. Consequently, this necessitates incorporating a very expensive, metal vacuum dewar into the system. Thermally activated ("thermal") batteries may provide a viable alternative to these systems. Thermal batteries that we develop commonly employ various molten-salt electrolytes with Li-alloy anodes (e.g., Li-Si) and metal-sulfide cathodes (e.g., FeS_2 and CoS_2). Such batteries are capable of high-rate pulses (>5 A/cm^2) (1).

It would be desirable to use a molten-salt based power supply for geothermal applications, since the geothermal borehole temperatures can easily exceed 300°C, and in some cases reach temperatures as high as 400°C. These conditions would seem applicable for a modified thermal battery. The possibility of using a molten-salt system for a geothermal-borehole power application was examined and evaluated in detail (2). Normally, a thermal battery requires an internal pyrotechnic heat source to bring the battery to operating temperatures, typically 450°C to 550°C. Thus, thermal management becomes critical for proper operation for any extended period (e.g., one hour or more). However, if the battery internal temperature can be sustained—by the appropriate internal pyrotechnics and proper thermal management—until the battery is in the hot (>300°C) zone of the borehole, then this concept might be viable with the proper electrolyte.

DISTRIBUTION OF THIS DOCUMENT IS UNLIMITED

MASTER

DTIC QUALITY INSPECTED 1

DISCLAIMER

This report was prepared as an account of work sponsored by an agency of the United States Government. Neither the United States Government nor any agency thereof, nor any of their employees, makes any warranty, express or implied, or assumes any legal liability or responsibility for the accuracy, completeness, or usefulness of any information, apparatus, product, or process disclosed, or represents that its use would not infringe privately owned rights. Reference herein to any specific commercial product, process, or service by trade name, trademark, manufacturer, or otherwise does not necessarily constitute or imply its endorsement, recommendation, or favoring by the United States Government or any agency thereof. The views and opinions of authors expressed herein do not necessarily state or reflect those of the United States Government or any agency thereof.

The standard electrolytes currently being used in our thermal batteries include the LiCl-KCl eutectic (m.p.=352°C), the minimum-melting LiCl-LiBr-LiF electrolyte (m.p.=436°C), and the low-melting LiBr-KBr-LiF eutectic (m.p.=324.5°C) (3). All have melting points above 300°C. However, there are other low-melting halide-based systems available, however, such as those based on Cs^+ and Rb^+ salts. The CsBr-LiBr-KBr eutectic, for example, is reported to melt at 236°C. The tetrachloroaluminates have also been examined in great detail for systems that use β"-Al_2O_3 Na^+-conducting ceramic separators and which operate at 300°C (4). There are a number of the tetrachloroaluminates that are liquid at room temperature. Wilkes *et al.* have studied the dialkylimidazolium chloroaluminate salts extensively (5).

During this study, we examined a number of low-melting electrolytes to determine the practical current densities that could be sustained over a temperature range that spanned the thermal window that could be expected in a geothermal borehole environment. This paper reports on the results of constant-currents tests with single cells based on the LiBr-KBr-LiF eutectic with a pyrite (FeS_2) cathode and anodes of LiSi and, to a more-limited extent, Al. Preliminary data for a CsBr-LiBr-KBr eutectic are also presented. Cells incorporating a reference electrode were also used, to assess the relative degree of polarization at the anode and cathode.

EXPERIMENTAL

Materials

The primary electrolyte studied was the LiBr-KBr-LiF eutectic (57.33%/42.0%/0.67%).[1] A limited number of tests were carried out with the CsBr-LiBr-KBr eutectic (42.75%/39.08%/18.17%). Using differential scanning calorimetry (DSC), we measured a melting point of 228.5°C. The eutectics were prepared by fusion of the appropriate amounts of vacuum-dried, reagent-grade ingredients in a quartz crucible at 400°C and then quenching in an Inconel tray.

The separator mixes were prepared by grinding the electrolytes, mixing with MgO (Merck Maglite 'S'), and then fusing at 400°C for 16 hours. The LiBr-KBr-LiF eutectic required 25% MgO and the CsBr-LiBr-KBr eutectic required 30%. The primary catholyte was prepared by blending 73.5% purified FeS_2 (American Mineral, –325+425 mesh) and 1.5% Li_2O with separator based on the LiBr-KBr-LiF eutectic. The catholyte with the CsBr-based separator contained 75% FeS_2 and no Li_2O. The purity of the FeS_2 pyrite was better than 98%, with the main impurities being gangue material (e.g., siliceous minerals). The anolytes consisted of a mixture of 80% Li-Si alloy (Eagle-Picher) and 20% electrolyte. The Li-Si alloy contained 44% Li and was –100+325 mesh in size. All preparations, processing, and handling operations with materials and parts were conducted in a dry room maintained at <3% relative humidity.

---

[1] All compositions are reported as weight percentage.

Test Cells

The anode, cathode, and separator mixes were cold pressed into 1.25". (31.8-mm)-diameter discs to ~75% of theoretical density. The mass of the LiSi anode was 0.9 g and that of the Al anode was 1.4 g. The separator masses were 1 g for the standard cells and 5.8 g for cells with reference-electrodes. The cathode mass was 1.03 g. The reference electrode was a silver wire immersed in a borosilicate-glass capillary tube filled with a 0.1m AgCl solution in the halide electrolyte under study. The reference electrode was inserted into a slot between two separator pellets. In some cases, a thin (0.001"-thick) Mo foil was placed between two separator pellets to served as a quasi-reference electrode. Cells were discharged at temperatures of 400°C to as low as 250°C for the CsBr-based electrolyte.

Apparatus

The pellets were assembled into cells that were tested under an applied pressure of 5.3 psig (36.5 kPa) between heated platens under constant-current conditions in a glovebox under high-purity argon (<1 ppm each O_2 and H_2O). The cell current was doubled for 1 s of each 60-s cycle to obtain internal-resistance information and determine the rate capabilities of the cells. The cells were discharged under computer control with a PAR Model 273A potentiostat in the programmable galvanostatic mode. The steady-state current was controlled by the output of a D/A card, while the pulse magnitude was established using a pulse generator (HP8116A). One channel of the DVM sampled the cell voltage and a second channel sampled the anode-reference voltage (when a reference electrode was used). Separate high-speed DVMs (HP3458A) were used to digitize the cell voltage and anode-reference voltage during the pulse. The cell discharge was terminated when the cell voltage dropped below 1.25 V.

RESULTS AND DISCUSSION

LiBr-KBr-LiF Eutectic

Figure 1 shows a typical discharge trace at 400°C for a steady-state current density of 63 mA/cm^2 for a cell with a reference electrode. The corresponding anode and cathode traces are also shown. The voltage transitions at 800 s and 2,100 s are clearly associated with the cathode, as the anode voltage remained relatively unchanged until the very end of the discharge. The voltage transitions coincide with the increase in cell resistance during discharge, as evident in Figure 2.

The first transition probably results from the higher resistance of the first phase that forms during discharge, $Li_3Fe_2S_4$.[2] This material, the so-called "Z" phase, has been identified as the first discharge phase by Tomczuk and coworkers in their extensive characterization of the Li-alloy/FeS_2 couple for potential electric-vehicle applications

[2] It should be noted here that the initial reduction of FeS_2 does not involve a transition of Fe(III) to Fe(II), but involves the sulfur. The active reductant under these conditions can be considered to be a polysulfide. [Structurally, pyrite is a simple cubic with octahedrally coordinated Fe(II) at the corners and face centers of the cubic unit cell. The are pairs of S atoms at opposing corners. (6)]

(7,8). The sequence of discharge of FeS_2 in LiCl-KCl eutectic is shown in equation 1 for equilibrium conditions:

$$FeS_2 \rightarrow Li_3Fe_2S_4 \rightarrow Li_{2+x}FeS_2\ (x\sim0.2) + Fe_{1-x}S \rightarrow Li_2FeS_2 \rightarrow Li_2S + Fe \qquad [1]$$

The conductivities of chemically synthesized $Li_3Fe_2S_4$ and Li_2FeS_2 (the so-called "X" phase) have been reported from room temperature to 440°C (9). The conductivity of the Z phase was 10^{-5} S/cm at 25°C, 10^{-3} S/cm at 200°C, 0.01 S/cm at 300°C, and 0.10 S/cm at 400°C. The conductivity of the X phase was 0.09 S/cm at 25°C, 1.6 S/cm at 200°C, 2.8 S/cm at 300°C, and 4.2 S/cm at 400°C—orders of magnitude greater. In comparison, the conductivity of natural pyrite can vary from 1 to 10 S/cm at room temperature (10).

Thus, the increase in resistivity of the cell during discharge is consistent with the appearance of the Z phase. After this phase begins to discharge, the cell resistance drops due to the lower resistance of a mixture of the next discharge phases, $Li_{2+x}FeS_2$ (x~0.2) + $Fe_{1-x}S$. The second increase in cell resistance may be associated with the formation of the X phase with a slightly higher resistance. The cell voltage transitions observed are also consistent with data reported by Tomczuk for FeS_2 in LiCl-KCl eutectic (7).

The capacities of the cathode at the voltage transitions observed in the cathode-reference trace (Figure 1) are less than one would calculate based on the transitions indicated in equation 1. The first transition near 800s corresponds to a FeS_2 consumption of ~406 coulombs, about 44% of the theoretical for the transition to the Z phase. Similarly, the transition at 2,100 s corresponds to a FeS_2 consumption of 1,068 coulombs, about 88% of theoretical for the X phase. These discrepancies reflect that fact that the cathode is undergoing parallel discharge reactions rather than clean consecutive ones at this current density; i.e., the Z phase is discharging before all the FeS_2 is completely reacted. Discharging at a lower current density would be expected to improve the FeS_2 utilization. In fact, when a cell was discharged at only 32 mA/cm^2, the FeS_2 utilization at the first voltage transition increased to 88%, while that for the second voltage transition remained about the same. These data indicate the kinetics or polarization for the $FeS_2 \rightarrow Li_3Fe_2S_4$ transition are much greater than for Li_2FeS_4 formation.

The anode-reference voltage trace (Figure 1) is fairly flat until near the end of discharge. The anode would be expected to show a transition near this time, based on the discharge sequence shown in equation 2 (11). Based on the masses of anode and cathode and the transitions shown in equations 1 and 2, the cells in this study were cathode limited (cathode:anode capacity=0.88).

$$Li_{13}Si_4 \rightarrow Li_7Si_3 \rightarrow Li_{12}Li_7 \qquad [2]$$

The voltage plateau in the anode-reference trace is associated with the constant-potential, two-phase region consisting of the starting material, $Li_{13}Si_4$, and the first discharge phase, Li_7Si_3. The transition to the next phase, $Li_{12}Si7$, should occur at 2,300 s, which is in

general agreement with the onset of a phase transition in the anode-reference voltage trace. In the previously mentioned cell discharge at 32 mA/cm^2, a sharp anode transition was observed where expected. The measured voltage change of ~125 mV for that test is much larger than the equilibrium value of 49 mV (11) because of polarization losses, including those (ohmic) associated with half the thickness of the separator.

Examination of the cell voltage response during pulsing provides valuable information as to the nature of the polarization processes. The cell voltage responses to the first pulse (at 60 s) and fifth pulse (at 300 s) are shown in Figure 3. The sharp square response indicates the bulk of the polarization (about 88%) is ohmic, with only some concentration polarization present at this current density (126 mA/cm^2). The amount of ohmic polarization remained relatively unchanged for the entire discharge (varying between 88 and 91%) to a cutoff voltage of 1.25 V. A plot of the percentage of total cell polarization due to the anode is shown in Figure 4 during cell discharge. These data show that the major polarization is *cathode* related throughout the discharge, with the minimum values being associated with the large increase in resistance of the first discharge phases at the cathode.

Figure 5 shows the cell voltage and anode-reference voltage traces during discharge of a similar cell but at 350°C and a steady-state current density of 50 mA/cm^2, with a pulse current density of 100 mA/cm^2. At the lower temperature, the cell could not sustain the higher steady-state current density (63 mA/cm^2) that was used for the 400°C test. The voltage drop at initiation of discharge was due to the cathode, but the polarization for the remainder of the discharge became increasingly anode dominated, especially near the end, where it reached 88%. The resistance associated with the discharge is shown in Figure 6. The resistance maxima that were so well defined at 400°C (Figure 2) were absent at the lower temperature, which was only about 25°C above the freezing point. Instead, the resistance began to continually increase after about 250 s, reaching a value over five times the maximum observed at 400°C. This is consistent with the onset of a gradual transition in the cell voltage (Figure 5) near this time.

The voltages for the cell are shown in Figure 7 for the first pulse (at 60 s) and fifth pulse (at 300 s). The response is similar to that observed at 400°C at the higher rate (Figure 3), except that there is a slight increase in the amount of concentration polarization. This is more noticeable during the fifth pulse. The bulk of the polarization was still ohmic (84% at the first pulse), although the percentage of cell polarization associated with the anode increased from 44% for the first pulse to over 88% by the 10th pulse (at 600 s). Thus, the rate limiting processes have changed in going from 400°C to 350°C, with the *anode* polarization dominating at the lower temperature. The ohmic contribution is related to the lower ionic conductivity of the immobilized separator layer at 350°C, while the concentration polarization is most likely a result of a Li^+ gradient at the anode separator interface. Or, it could also be associated with slower diffusion of Li in the bulk alloy itself.

CsBr-LiBr-KBr Eutectic

Similar cell testing is underway with the CsBr-LiBr-KBr eutectic electrolyte, which has a much lower melting point than the LiBr-KBr-LiF eutectic. Preliminary results at 250°C–350°C indicate a rapid drop-off in capacity with decreasing temperature, along with a progressively increase with cell resistance. The resistance continued to increase during discharge rather than returning to a value similar to the starting one, much as was observed with the LiBr-KBr-LiF eutectic-based cells at 350°C. This is, in part, a consequence of the higher resistivity of the separator based on the CsBr-LiBr-KBr eutectic. At 350°C, for example, the resistivity of the separator with CsBr-LiBr-KBr eutectic is 14.4 ohm-cm, while that of the separator with LiBr-KBr-LiF eutectic is only 1.9 ohm-cm (12). Also, as the temperature is lowered, the kinetics of the charge-transfer processes will become increasingly sluggish. The investigation of the CsBr-based electrolyte is continuing and will involve the use of additional characterization techniques such as cyclic voltammetry and complex-impedance spectroscopy..

CONCLUSIONS

The kinetics of the discharge processes in LiSi/LiBr-KBr-LiF/FeS_2 single cells with immobilized electrolyte were examined under constant-current conditions. At 400°C under a steady-state load of 63 mA/cm^2, the bulk of the cell polarization is ohmic and cathode related. The cell voltage transitions that are observed are associated with phase changes in the cathode. The first maximum in cell resistance during discharge is attributed to the formation of $Li_3Fe_2S_4$ which has a much higher resistivity than FeS_2. The second (smaller) resistance peak is likely due to the formation of Li_2FeS_2, which is less resistive. The cell resistance at the end of discharge is similar to that at the start of the test.

At 350°C, the LiSi/LiBr-KBr-LiF/FeS_2 couple cannot support a sustained current density of 64 mA/cm^2, but can perform well at 50 mA/cm^2. At the lower temperature, the polarization becomes increasingly dominated by the anode. The distinct phase transformation (voltage transitions) observed at 400°C are not evident at 350°C, with only a single weak transition being seen. The cell resistance gradually increases during discharge, reaching a value over five times that at for the 400°C cell.

Preliminary work with the LiSi/FeS_2 couple with the lower-melting CsBr-LiBr-LiF eutectic (melting point=228.5°C) indicates a considerable degradation in cell performance relative to the LiBr-KBr-LiF eutectic. The capacity is considerably reduced and the cell resistance increases by more than a factor of seven, due to the higher resistivity of the electrolyte. More work is underway to characterize this system more fully.

Preliminary work with the LiSi/FeS_2 couple with the lower-melting CsBr-LiBr-LiF eutectic (melting point=228.5°C) indicates a considerable degradation in cell performance relative to the LiBr-KBr-LiF eutectic. The capacity is considerably reduced and the cell resistance increases by more than a factor of seven, due to the higher resistivity of the electrolyte. More work is underway to characterize this system more fully.

ACKNOWLEDGMENTS

Sandia National Laboratories is a multiprogram laboratory operated by Sandia Corp., a Lockheed Martin company, for the United States Department of Energy under Contract DE-AC04-94AL85000.

REFERENCES

1. Ronald A. Guidotti and Frederick W. Reinhardt, Proc. 19th Intern. Power Sources Symp , 443 (1995).
2. Randy A. Normann and Ronald A. Guidotti, Trans. of Geothermal Resources Council, Vol. **20**, 509 (1996).
3. R. A. Guidotti and F. W. Reinhardt, Proc. 33rd Power Sources Symp., 369 (1988).
4. J. Caja, Proc. 17th Intern. Power Sources Symp., 333 (1991).
5. T. L. Riechel and J. S. Wilkes, J. Electrochem. Soc., **139** (4), 977 (1992).
6. K. K. Mishra and K. Osseo-Asare, J. Electrochem. Soc., **135** (10),2502 (1988).
7. Z. Tomczuk, B. Tani, N. C. Otto, M. F. Roche, and D. R. Vissers, J. Electrochem. Soc., **129** (5), 925 (1982) (and references therein).
8. S. K. Preta, Z. Tomczuk, S. von Winbush, and M. F. Roche, J. Electrochem. Soc., **130** (2), 264 (1983).
9. S. P. S. Badwal and R. J Thorn, J. Sol. St. Chem.**43**, 167 (1982).
10. S. Fiechter, M. Birkholz, A. Hartmann, P. Dulski, Giersig, H. Tributsch, and R. J. D. Tilley, J. Mater. Res., 7 (7), 1829 (1992).
11. C. J. Wen and R. A. Huggins, J. Sol. St. Chem. **37**, 271 (1981).
12. L. Redey, M. McParland, and R. Guidotti, Proc. 34th Power Sources Symp., 128 (1990).

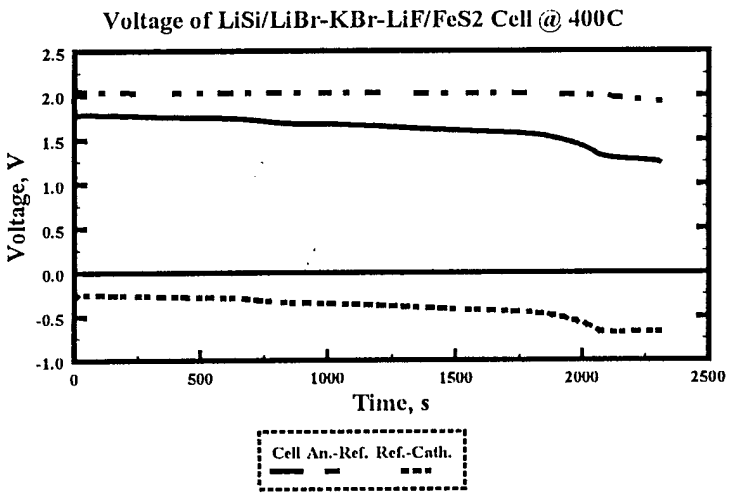

Figure 1. Response of LiSi/LiBr-KBr-LiF/FeS2 Cell at 400C Under Stateady-State Load of 63 mA/sq cm.

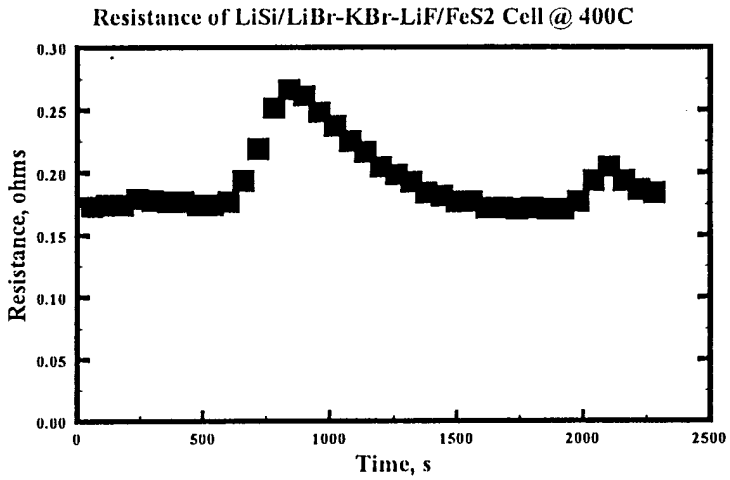

Figure 2. Resistance of LiSi/LiBr-KBr-LiF/FeS2 Cell at 400C During Discharge Under Steady-State Load of 63 mA/sq cm.

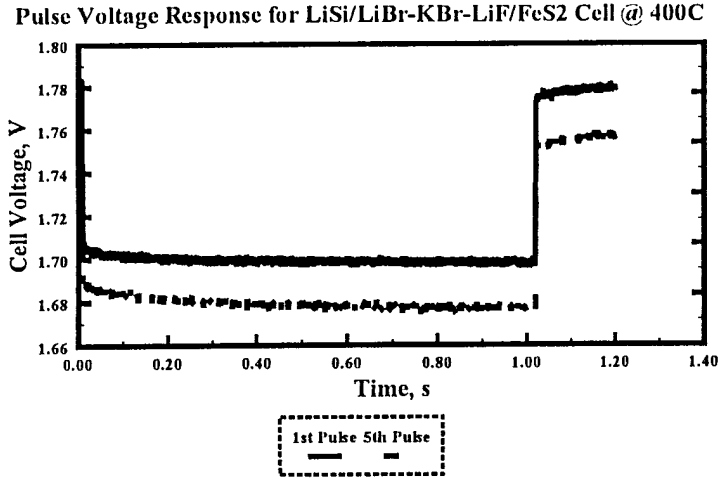

Figure 3. Pulse Response of LiSi/LiBr-KBr-LiF/FeS2 Cell at 400C During Pulse of 125 mA/sq cm.

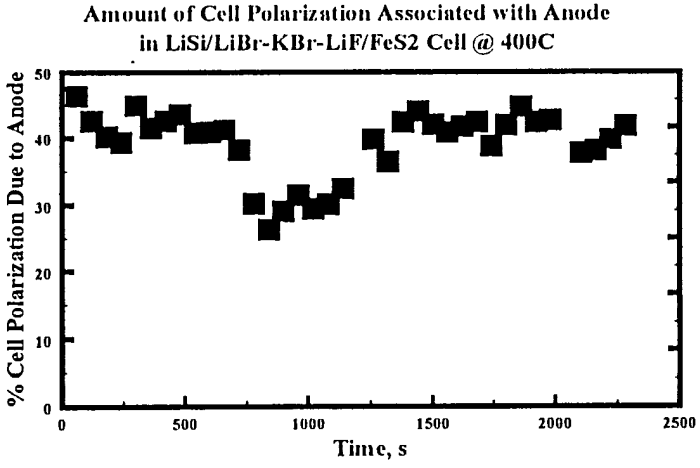

Figure 4. Relative Anode Polarization of LiSi/LiBr-KBr-LiF/FeS2 Cell at 400C at 63 mA/sq cm.

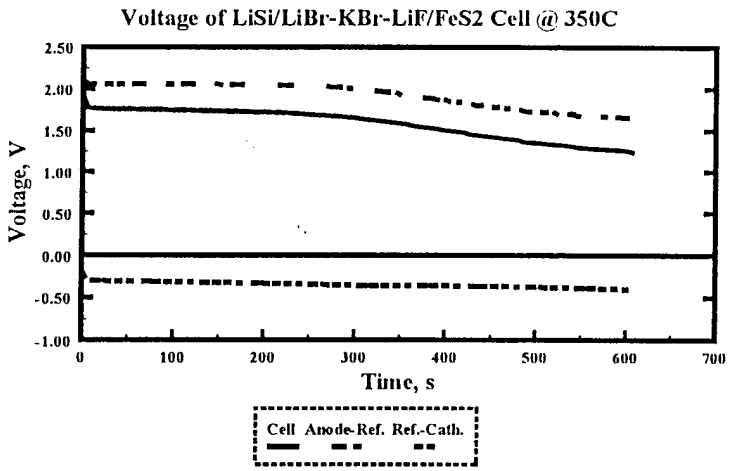

Figure 5. Response of LiSi/LiBr-KBr-LiF/FeS2 Cell at 350C Under Steady-State Load of 50 mA/sq cm.

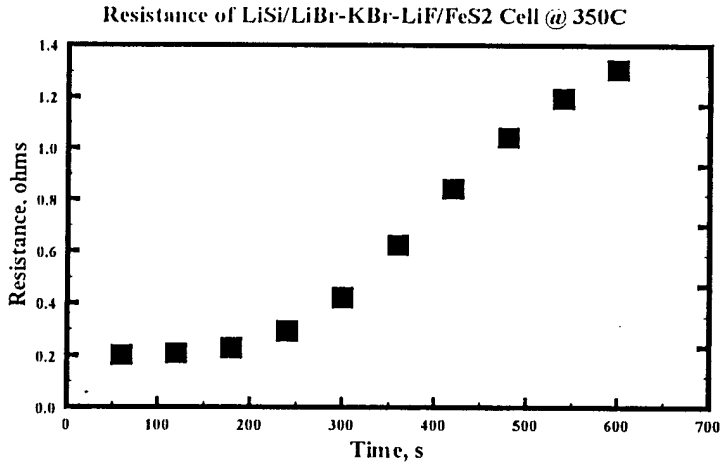

Figure 6. Resistance of LiSi/LiBr-KBr-LiF/FeS2 Cell at 350C During Discharge Under Steady-State Load of 50 mA/sq cm.

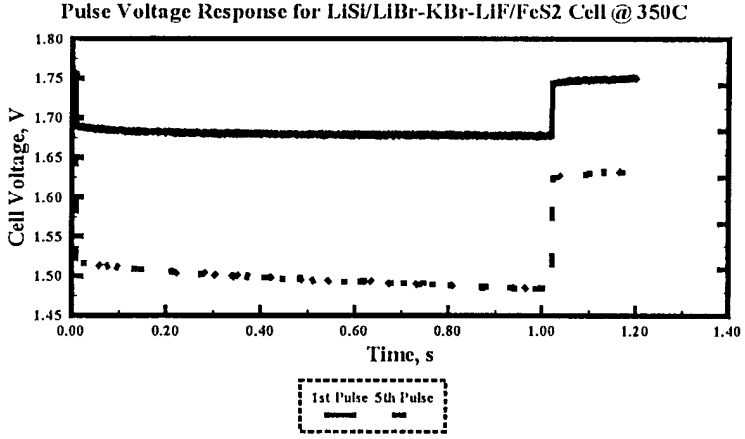

Figure 7. Response of LiSi/LiBr-KBr-LiF/FeS2 Cell at 350C During Pulse of 100 mA/sq cm.

M98005458

Report Number (14) SAND--98-1105C
CONF-980504--

Publ. Date (11) 199805
Sponsor Code (18) DOE/EE, XF
UC Category (19) UC-1240, DOE/ER

19980706 051

DOE